Electronic Supplementary Information

Experimental Section

Materials: Sodium nitrite ($NaNO_2$, 99.9%), ammonium chloride (NH_4Cl), sodium hydroxide (NaOH), sodium salicylate ($C_7H_5NaO_3$), trisodium citrate dehydrate ($C_6H_5Na_3O_7 \cdot 2H_2O$), p-dimethylaminobenzaldehyde ($C_9H_{11}NO$), sodium nitroferricyanide dehydrate ($C_5FeN_6Na_2O \cdot 2H_2O$) and sodium hypochlorite solution (NaClO) were purchased from Aladdin Co., Ltd. (Shanghai, China). Sulfuric acid (H_2SO_4), hydrogen peroxide (H_2O_2), hydrochloric acid (HCl), acetone hydrazine monohydrate ($N_2H_4 \cdot H_2O$), and ethanol were bought from Beijing Chemical Corporation. (China). Silver nitrate ($Ag(NO_3)_2 \cdot 6H_2O$, >98%) was purchased from Chengdu Kelong Chemical Regent Co. Ltd. Titanium plate (TP, 0.4 mm thick) was purchased from Qingyuan Metal Materials Co., Ltd (Xingtai, China). All reagents used in this work are analytical grade without further purification.

Preparation of Ag@TiO_2/TP: TP (2.0 × 3.0 cm^2) was firstly sonicated in HCl, acetone, and water for 10 min, respectively. The pretreated TP was then put into 5 M NaOH solutions in Teflon-lined autoclave and heated at 180°C for 24 h to get $Na_2Ti_2O_5$/TP. Subsequently, the obtained $Na_2Ti_2O_5$/TP was immersed in 0.1 M $Ag(NO_3)_2 \cdot 6H_2O$ for 10 h to exchange Na^+ with Ag^+, followed by washing with water and dried. Finally, $AgTi_2O_5$/TP was annealed at 500°C for 2h under Ar/H_2 atmosphere, and Ag@TiO_2/TP was eventually obtained. As a control, TiO_2/TP was synthesized by the identical fabrication process of Ag@TiO_2/TP, but immersing the $Na_2Ti_2O_5$/TP into diluted HCl to exchange Na^+ to H^+.

Characterizations: X-ray diffraction (XRD) data were acquired by diffraction instrument with a Cu Kα radiation (Shimadzu XRD-6100). SEM measurements were carried out on a GeminiSEM 300 scanning electron microscope (ZEISS, Germany) at an accelerating voltage of 5 kV. TEM image was gotten by a Zeiss Libra 200FE transmission electron microscope operated at 200 kV. X-ray photoelectron spectroscopy (XPS) data were acquired by an X-ray photoelectron spectrometer

(ESCALABMK II) with Mg as the exciting source. UV–vis spectrophotometer (Shimadzu UV-1800) was used to gain the absorbance data. Gas chromatography analysis was performed on a Shimadzu GC-2014C with Ar as carrier gas.

Electrochemical measurements: The electrolysis was performed in an H-type cell separated by a Nafion 117 membrane, using Ag@TiO_2/TP (1 ×0.5 cm^2) as the working electrode with a CHI 660E electrochemical workstation (Shanghai, Chenhua). A commercial graphite rod and Hg/HgO were used as counter and reference electrodes. The two compartments of H-type cell were filled with 35 mL Ar-saturated electrolyte solution (0.1 M NaOH with and without 0.1 M NO_2^-). The curves of linear sweep voltammetry (LSV) were recorded at a scan rate of 10 mV s^{-1} from 0.2 to −0.8 V. The chronoamperometry was conducted at different potentials and cycle tests for 1 h, and the stability tests for 12-h. All potentials reported in our work were converted to reversible hydrogen electrode via calibration with the following equation: E (RHE) = E (Hg/HgO) + (0.098+0.0591×pH) V.

Determination of NH_3: The NH_3 concentration in the solution was determined by colorimetry (the obtained electrolyte was diluted 40 times) using the indophenol blue method.[1] In detail, 2 mL of the solution after reaction was mixed with 2 mL of 1 M NaOH coloring solution containing 5% $C_7H_5NaO_3$ and 5% $C_6H_5Na_3O_7 \cdot 2H_2O$. Then, 1 mL oxidizing solution of 0.05 M NaClO and 0.2 mL catalyst solution of $C_5FeN_6Na_2O$ (1 wt%) were added to the above solution. After standing in the dark for 2 h, the UV–vis absorption spectra were measured. The concentration of NH_3 was identified using the absorbance at a wavelength of 655 nm. The concentration-absorbance curve was calibrated using the standard NH_4Cl solution with NH_3 concentrations of 0.2, 0.5, 1.0, 2.0, 5.0 and 10.0 ppm in 0.1 M NaOH solution. The fitting curve (y =0.377 x+0.06791, R^2=0.99794) shows good linear relation of absorbance value with NH_3 concentration.

Determination of N_2H_4: The N_2H_4 was estimated by the Watt and Chrisp method.[2] The color reagent was a solution of 18.15 mg mL^{-1} of $C_9H_{11}NO$ in the mixed solvent of HCl and ethanol (V/V: 1/10). In detail, 2 mL electrolyte was added into 2 mL color

reagent for 15 min under stirring. The absorbance of such solution was measured to quantify the hydrazine yields by the standard curve of hydrazine ($y = 0.69 x + 0.0658$, $R^2 = 0.99989$).

Determination of N_2 and H_2: N_2 and H_2 were quantified by gas chromatography (GC).

Calculations of NH_3 FE and NH_3 yield:

The amount of NH_3 (m_{NH3}) was calculated by the following equation:

$$m_{NH3} = [NH_3] \times V$$

NH_3 FE was calculated by the following equation:

$$FE = (6 \times F \times [NH_3] \times V) / (M_{NH3} \times Q) \times 100\%$$

NH_3 yield was calculated using the following equation:

$$NH_3 \text{ yield} = ([NH_3] \times V) / (M_{NH3} \times t \times A)$$

Where F is the Faraday constant (96485 C mol^{-1}), $[NH_3]$ is the NH_3 concentration, V is the volume of electrolyte in the anode compartment (35 mL), M_{NH3} is the molar mass of NH_3 molecule, Q is the total quantity of applied electricity, t is the electrolysis time (1 h), and A is the geometric area of the working electrode (1 × 0.5 cm^2).

The partial current density of NH_3 (jNH_3) was calculated as:

$$jNH_3 = FE_{NH3} \times I_{it}$$

where I_{it} is the average current density (mA cm^{-2}) during the potentiostatic tests at given potentials.

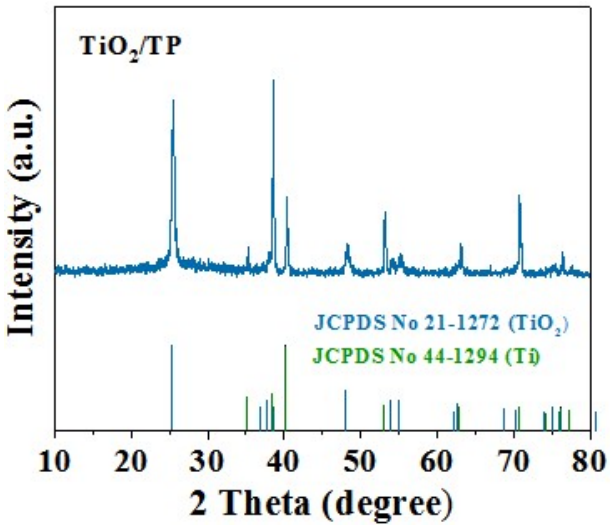

Fig. S1. XRD pattern of TiO_2/TP.

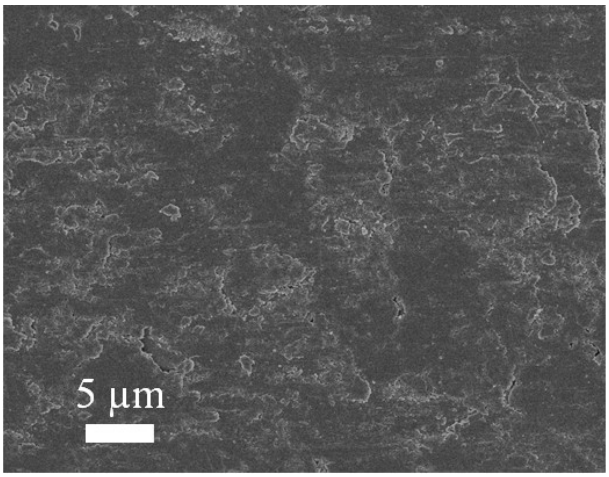

Fig. S2. SEM image of TP.

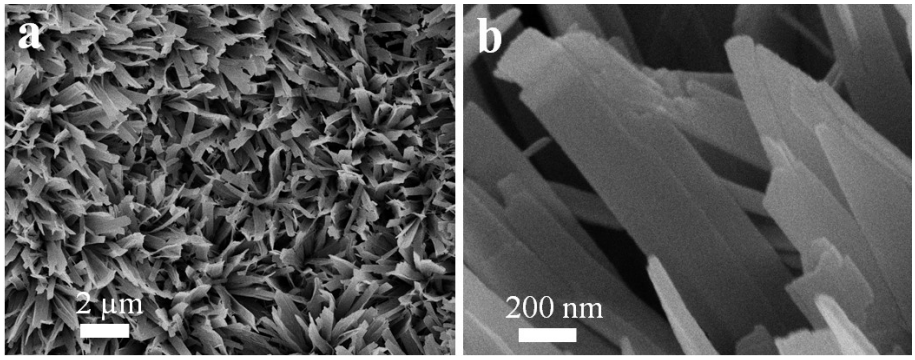

Fig. S3. SEM images of TiO_2/TP.

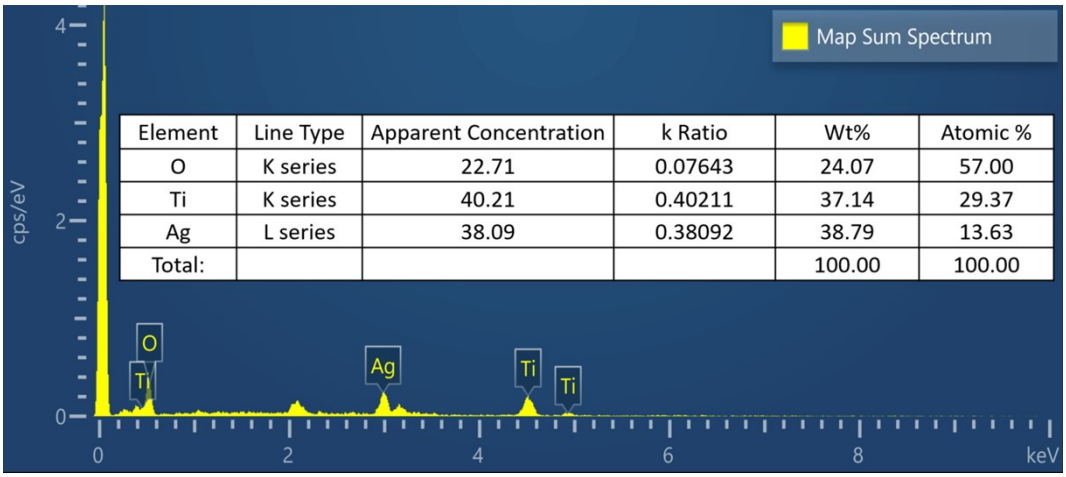

Element	Line Type	Apparent Concentration	k Ratio	Wt%	Atomic %
O	K series	22.71	0.07643	24.07	57.00
Ti	K series	40.21	0.40211	37.14	29.37
Ag	L series	38.09	0.38092	38.79	13.63
Total:				100.00	100.00

Fig. S4. EDX spectrum of Ag@TiO_2/TP.

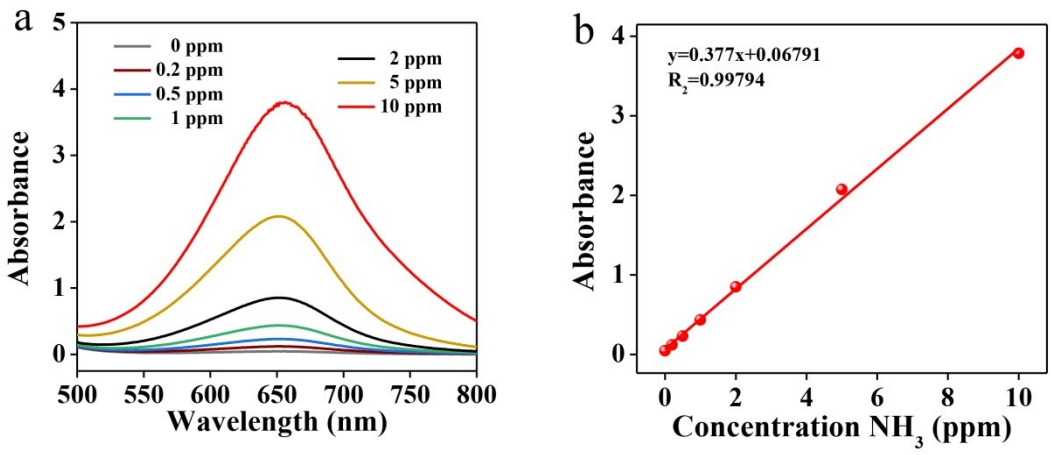

Fig. S5. (a) UV–vis absorption spectra and (b) corresponding calibration curve used for calculation of NH_3 concentration.

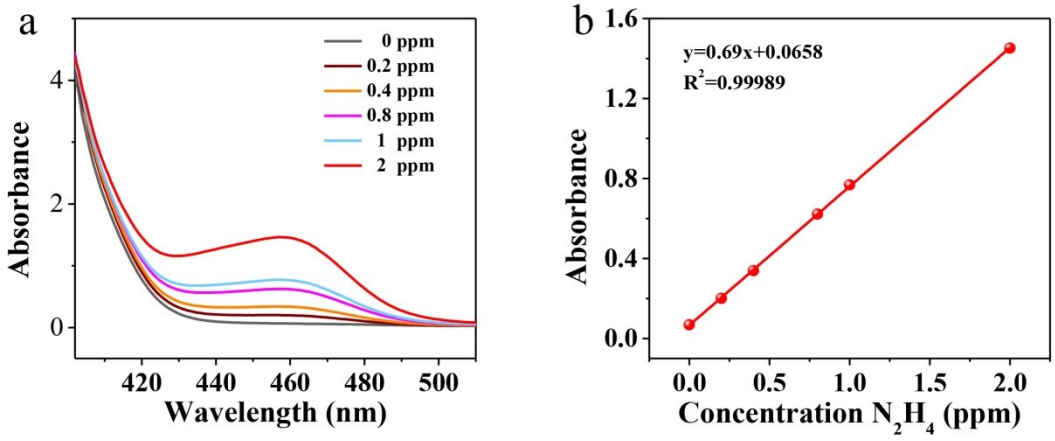

Fig. S6. (a) UV–vis absorption spectra and (b) corresponding calibration curve used for calculation of N_2H_4 concentration.

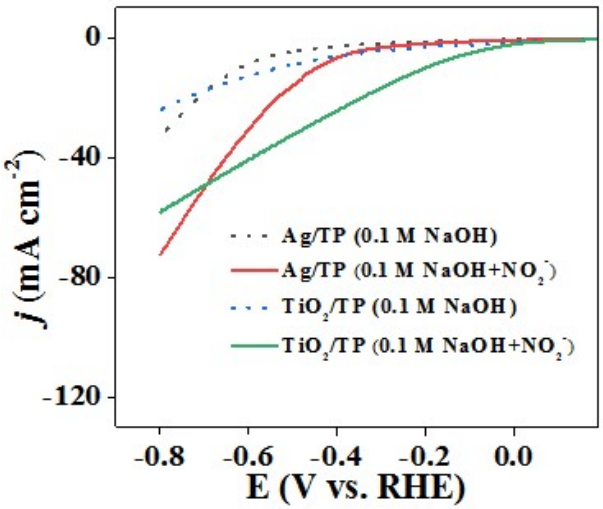

Fig. S7. LSV curves of TiO_2/TP and Ag/TP in 0.1 M NaOH with/without 0.1 M NO_2^-.

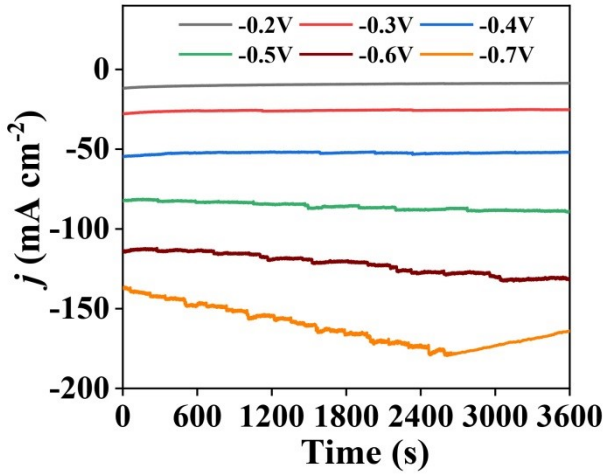

Fig. S8. Chronoamperometry curves of Ag@TiO_2/TP for the NO_2^-RR at different applied potentials.

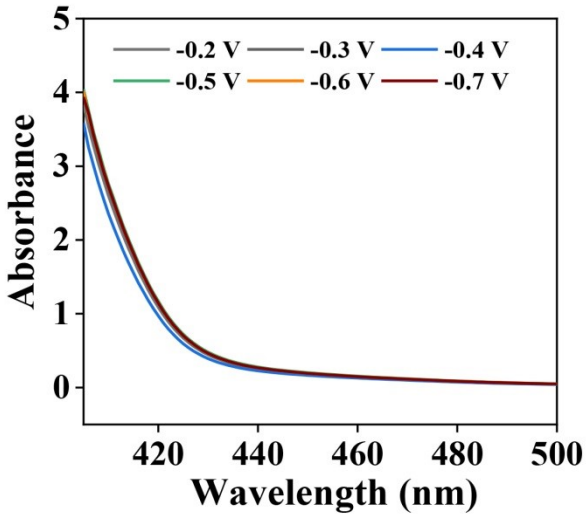

Fig. S9. UV–vis absorption spectra of N_2H_4 of $Ag@TiO_2$/TP at different given potentials.

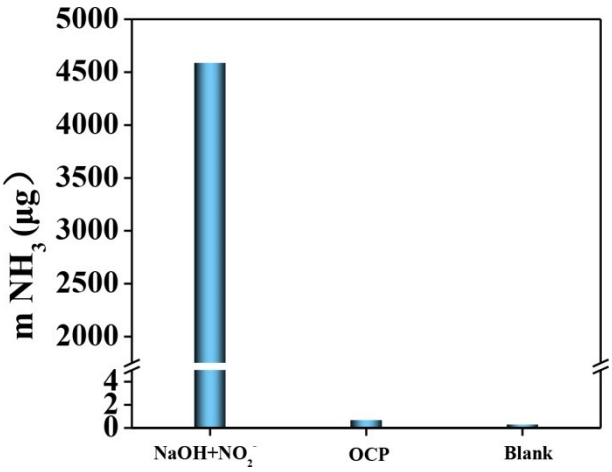

Fig. S10. NO_2^-RR performance of Ag@TiO_2/TP under different test conditions.

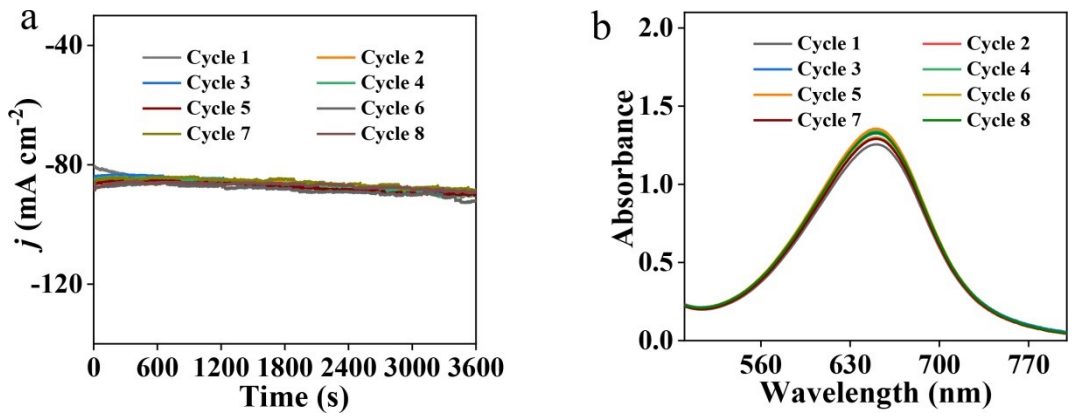

Fig. S11. (a) CA curves and (b) corresponding UV–vis spectra of Ag@TiO_2/TP for NH_3 generation during recycling tests at –0.5 V.

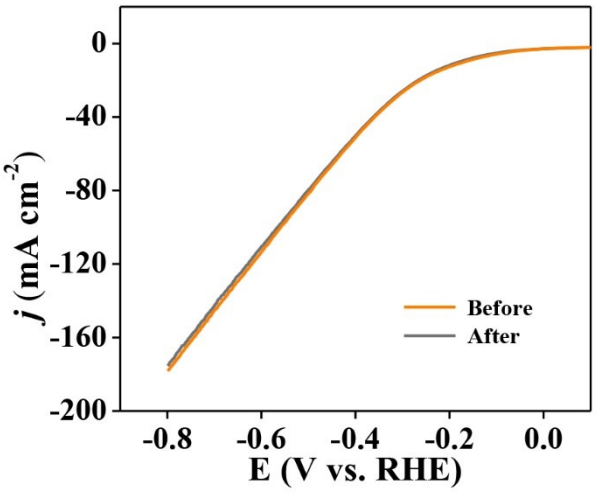

Fig. S12. LSV curves of Ag@TiO_2/TP in 0.1 M NaOH with 0.1 M NO_2^- before and after long-time electrolysis.

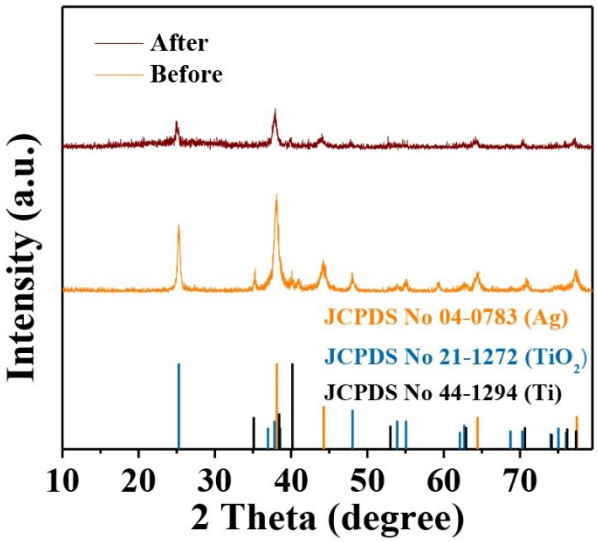

Fig. S13. XRD patterns of Ag@TiO_2/TP before and after long-time electrolysis.

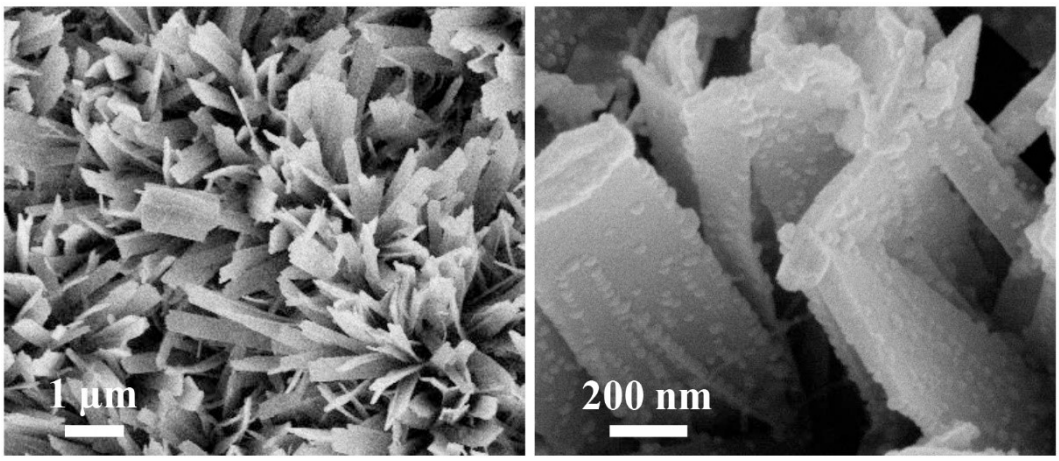

Fig. S14. SEM images of Ag@TiO_2/TP after long-time electrolysis.

Table S1. Comparison of NH_3 yield and FE of Ag@TiO_2/TP with other reported NO_2^-RR electrocatalysts.

Catalyst	Electrolyte	NH_3 yield ($\mu g\ h^{-1}\ cm^{-2}$)	FE (%)	Potential (V vs. RHE)	Ref
Ag@TiO_2/TP	0.1 M NaOH (0.1 M NO_2^-)	8,743.1	96.4	–0.50	This work
Ag@NiO/CC	0.1 M NaOH (0.1 M NO_2^-)	5,751	96.1	–0.70	3
TiO_{2-x}	0.1 M NaOH (0.1 M NO_2^-)	7,898	92.7	–0.70	4
P-TiO_2	0.5 M Na_2SO_4 (50 ppm NO_3^-)	9,533.6	90.6	–0.60	5
CoB nanoarray	0.2 M Na_2SO_4 (400 ppm NO_2^-)	3,962.7	3,962.7	–0.70	6
MnO_2 nanoarrays	0.1 M Na_2SO_4 (5 mM NO_2^-)	1.46×10^{-10}	6	−1.75	7
Ni-NSA-V_{Ni}	0.2 M Na_2SO_4 (200 ppm NO_2^-)	4,011.7	96.1	−0.54	8
Cu_3P NA/CF	0.1 M PBS (0.1 M NO_2^-)	1,626.6	91.2 ± 2.5	−0.50	9
Ni@MDC	0.1 M NaOH (0.1 M NO_2^-)	5,100	65.4	−0.80	10

References

1 R. E. Ruther, R. J. Hamers, Photo-illuminated diamond as a solid-state source of solvated electrons in water for nitrogen reduction, *Nat. Mater*., 2013, **12**, 836–841.

2 L. C. Green, D. A. Wagner, J. Glogowski, P. L. Skipper, J. S. Wishnok, S. R, Tannenbaum, Analysis of nitrate, nitrite, and [^{15}N] nitrate in biological fluids, *Anal. Biochem*., 1982,**126**, 131–138.

3 Q. Liu, G. Wen, D. Zhao, L. Xie, S. Sun, L. Zhang, Y. Luo, A. A. Alshehri, M. S. Hamdy, Q. Kong, X. Sun, Nitrite reduction over Ag nanoarray electrocatalyst for ammonia synthesis, *J. Colloid Interface Sci*., 2022, **623**, 513–519.

4 D. Zhao, J. Liang, J. Li, L. Zhang, K. Dong, L. Yue, Y. Luo, Y. Ren, Q. Liu, M. S. Hamdy, Q. Kong, Q. Liu, X. Sun, A TiO_{2-x} nanobelt array with oxygen vacancies: an efficient electrocatalyst toward nitrite conversion to ammonia, *Chem. Commun*., 2022, **58**, 3669–3672.

5 L. Ouyang, X. He, S. Sun, Y. Luo, D. Zheng, J. Chen, Y. Li, Y. Lin, Q. Liu, A. M. Asirif, X. Sun, Enhanced electrocatalytic nitrite reduction to ammonia over P-doped TiO_2 nanobelt array, *J. Mater. Chem. A*, 2022, **10**, 23494–23498.

6 L. Hu, D. Zhao, C. Liu, Y. Liang, D. Zheng, S. Sun, Q. Li, Q. Liu, Y. Luo, Y. Liao, L. Xie, X. Sun, Amorphous CoB nanoarray as a high-efficiency electrocatalyst for nitrite reduction to ammonia, *Inorg. Chem. Front*., 2022, **9**, 6075–6079.

7 R. Wang, Z. Wang, X. Xiang, R. Zhang, X. Shi, X. Sun, MnO_2 nanoarrays: an efficient catalyst electrode for nitrite electroreduction toward sensing and NH_3 synthesis applications, *Chem. Commun*., 2018, **54**, 10340–10342.

8 C. Wang, W. Zhou, Z. Sun, Y. Wang, B. Zhang, Y. Yu, Integrated selective nitrite reduction to ammonia with tetrahydroisoquinoline semi-dehydrogenation over a vacancy-rich Ni bifunctional electrode, *J. Mater. Chem. A*, 2021, **9**, 239–243.

9 J. Liang, B. Deng, Q. Liu, G. Wen, Q. Liu, T. Li, Y. Luo, A. A. Alshehri, K. A. Alzahrani, D. Ma, X. Sun, High-efficiency electrochemical nitrite reduction to ammonium using a Cu_3P nanowire array under ambient conditions, *Green Chem*., 2021, **23**, 5487–5493.

10 X. He, X. Li, X. Fan, J. Li, D. Zhao, L. Zhang, S. Sun, Y. Luo, D. Zheng, L. Xie, A. M. Asiri, Q. Liu, X. Sun, Ambient electroreduction of nitrite to ammonia over Ni nanoparticle supported on molasses-derived carbon sheets, *ACS Appl. Nano Mater*., 2022, **5**, 14246−14250.